NASA-26:3205

COMPLETED

ORIGINAL

NASA Contractor Report 3205

An Improved Woodward's Panel Method for Calculating Leading-Edge and Side-Edge Suction Forces at Subsonic and Supersonic Speeds

C. Edward Lan and Sudhir C. Mehrotra

GRANT NSG-1046
NOVEMBER 1979

NASA

37

NASA Contractor Report 3205

An Improved Woodward's Panel Method for Calculating Leading-Edge and Side-Edge Suction Forces at Subsonic and Supersonic Speeds

C. Edward Lan and Sudhir C. Mehrotra
University of Kansas Center for Research, Inc.
Lawrence, Kansas

Prepared for
Langley Research Center
under Grant NSG-1046

NASA
National Aeronautics
and Space Administration

Scientific and Technical
Information Branch

1979

a

side-edge suction force. Examination of the two-dimensional flat plate problem indicated that if a constant-percent control point location is used, the overall force and moment and the pressure distribution cannot be accurately predicted simultaneously. Originally, Woodward (ref. 1) recommended 95% of the panel chord as the suitable location for the control point. Later, 95% location was corrected based on calculating the two-dimensional lift of flat plate (refs. 3,4). However, 95% location for supersonic but does not produce accurate pressure distribution and pitching moment.

Recently, Ehlers and Woolard (ref. 5) developed a method to calculate the leading-edge and side-edge suction in supersonic flow. After the strengths of the panel singularity have been obtained, they replaced them by a system of equivalent concentrated vortices. The surface flow are then calculated by applying Kutta-Joukowski law at the edges. Integration along the planform edges. Only [illegible] compared with other known theoretical solutions.

In this report, a new method to [illegible] will be described. The pressure prediction is based on [illegible] theory. The method used in reference 6 is then applied to calculate leading-edge and side-edge suction forces by [illegible] pressure distribution. The method is applicable to [illegible] supersonic flow.

SYMBOLS

A	aspect ratio
C	leading-edge suction parameter (see equation 4.3)
C_L	total lift coefficient
c	chord length

c_{d_i} sectional induced drag coefficient

c_ℓ sectional lift coefficient

c_m sectional pitching moment coefficient about local leading edge

c_r root chord

c_{ref} reference chord

c_s sectional leading-edge suction coefficient

c_t sectional leading-edge thrust coefficient

h/c maximum camber height to chord ratio

$\vec{I},\vec{J},\vec{K}$ unit vectors along x-, y- and z-axes, respectively

K_p planform lift curve slope per radian at $\alpha = 0^\circ$

$K_{v,le}$ leading-edge suction coefficient at one radian angle of attack

$K_{v,te}$ side-edge suction coefficient at one radian angle of attack

M Mach number

N_c number of chordwise panels

N_s number of spanwise strips

s distance from the leading-edge along the camber line nondimensionalized with respect to the local chord

S_s side-edge suction force per unit length of tip chord

x,y,z wind-fixed rectangular coordinates with positive x-axis along axis of symmetry pointing downstream, positive y-axis pointing to right, and positive z-axis pointing upward

x_{cp} x- coordinate of center of pressure

x_{le} x-coordinate of the leading-edge

$z_c(\zeta)$ camber function

α angle of attack

δ_c $= \tan^{-1}\left(\frac{\partial z_c}{\partial \zeta}\right)$

δ_f flap angle

δ_o = δ_c at the leading edge

Γ accumulated vortex strength defined by Eq. (28)

γ vortex density

Λ leading-edge sweep angle

λ taper ratio

ξ = $(x-x_\ell)/c$

THEORETICAL DEVELOPMENT

Airfoils

Planar

The main objective in the initial development is to predict exactly the pressure distribution of a flat-plate airfoil at those locations such that the lift and moment coefficients can be easily obtained by integrating the pressure. According to the Quasi-Vortex-Lattice Method (QVLM) (Ref. 1), these locations are best to be given by the cosine law distribution:

$$\xi_k = (1 - \cos((2k - 1)\pi/2N_c))/2, \quad k = 1, \ldots, N_c \tag{1}$$

where N_c is the number of chordwise panels and chord length is assumed to be unity. The chordwise paneling scheme will be based on the following cosine law:

$$\xi_{j+1} = (1 - \cos(j\pi/N_c))/2, \quad j = 0, 1, \ldots, N_c \tag{2}$$

Assuming the angle of attack to be one radian, the airfoil integral equation can be written as

$$4\pi = \int_0^1 \frac{\Delta C_p(\xi')d\xi'}{\xi - \xi'} \tag{3}$$

If the chord is divided into N_c segments on each of which ΔC_p is assumed constant, equation (3) can be integrated over each segment to give

$$4\pi = \sum_{j=1}^{N_c} \Delta C_p(\xi_k)\ln|(\xi_j - \xi_i)/(\xi_{j+1} - \xi_i)|, \quad i = 1, \ldots, N_c \tag{4}$$

where ξ_i is the control point location and $\xi_j < \xi_k < \xi_{j+1}$. Equation (4) will now be used to find ξ_i such that the predicted $\Delta C_{p_k} = \Delta C_p(\xi_k)$ will be exact. Since the problem is a nonlinear one, it can be solved by the following iterative method. Differentiating equation (4) with respect to ξ_i gives

$$\sum_{j=1}^{N_c} \frac{\partial \Delta C_{p_k}}{\partial \xi_i} \ln|\frac{\xi_j - \xi_i}{\xi_{j+1} - \xi_i}| = -\sum_{j=1}^{N_c} \Delta C_{p_k} [\frac{1}{\xi_{j+1} - \xi_i} - \frac{1}{\xi_j - \xi_i}], \quad i = 1, \ldots, N_c \tag{5}$$

Solving equation (5) will result in a set of $\partial \Delta C_{pk}/\partial \xi_i$ - values. If $\Delta C_{p_k}^{(d)}$ is the desired value and $\Delta C_{p_k}^{(c)}$ is the computed one, an incremental change in control point location $\Delta \xi_i$ can be obtained from

$$\sum_{i=1}^{N_c} \frac{\partial \Delta C_{p_k}}{\partial \xi_i} \Delta \xi_i = \Delta C_{p_k}^{(d)} - \Delta C_{p_k}^{(c)}, \quad k=1, \ldots, N_c \tag{6}$$

If the starting ξ_i is chosen at 95% of panel chord, four or five iterations can produce essentially exact solution. Once ΔC_{p_k} are obtained, the lift coefficient is computed as

$$c_\ell = \int_0^1 \Delta C_p d\xi = \frac{1}{2}\int_0^\pi \Delta C_p \sin\theta d\theta \approx \frac{1}{2}\frac{\pi}{N_c}\sum_{k=1}^{N_c} \Delta C_{p_k} \sin\theta_k \tag{7}$$

Similar expression for C_{p_2} can be derived. With the resultant load distribution, the lending edge suction and the moment at the quarter-chord

Cambered Airfoils

The control points found by the above method can be used directly for cambered airfoils. In this case, the flow tangency condition to be satisfied is developed as follows. Let the camber shape be described by

$$z(\xi,z) = z - z_c(\xi) = \qquad (8)$$

The flow tangency condition is then given by

$$(V_\infty \cos\alpha \vec{i} + V_\infty \sin\alpha \vec{k} + u\vec{i} + w\vec{k}) \cdot (-\frac{\partial z_c}{\partial \xi}\vec{i} + \vec{k}) = 0 \qquad (9)$$

or, in linearized form,

$$\frac{w}{V_\infty} = \frac{1}{4\pi}\int_0^1 \frac{\Delta C_p(\xi')d\xi'}{\xi' - \xi} = -\sin\alpha + \cos\alpha \frac{\partial z_c}{\partial \xi} \qquad (10)$$

After ΔC_p is calculated by satisfying equation (10), the aerodynamic forces can be calculated by resolving in the appropriate direction the pressure force which is assumed to act normal and along the vortex line. According to the incompressible Bernoulli equation, the pressure coefficient for lift at high α, C_p', is related to C_p at small α as follows:

$$C_p' = 1 - \frac{1}{V_\infty^2}[(V_\infty\cos\alpha + u)^2 + (V_\infty\sin\alpha + w)^2] - (\cos\alpha)u \qquad (11)$$

$$= (\cos\alpha)C_p$$

It follows that

$$\Delta C_l' = (\cos\alpha)\Delta C_l \tag{12}$$

where ΔC_l is calculated through equation (10). According to Figure 1, the aerodynamic characteristics are given by the following equations:

$$c_n = \int_0^1 \Delta C_l \cos\alpha \, d(x - \delta_x) + c_{l_0} \sin(\alpha - \delta_\alpha)$$

$$= \int^1 \Delta C_l \cos\alpha \frac{d(x - \delta_x)}{d\xi} d\xi + c_{l_0} \sin(\alpha - \delta_\alpha) \tag{13}$$

$$c_a = \int^1 \Delta C_l \sin\alpha \frac{d(x - \delta_x)}{d\xi} d\xi - c_{l_0} \cos(\alpha - \delta_\alpha) \tag{14}$$

$$c_{m_{le}} = -\int^1 \Delta C_l \left[\cos\alpha (x - \delta_x) + \sin\alpha (z - \delta_z)\right] d\left(\frac{x}{c}\right) - c_{m_0} \tag{15}$$

where $\delta_\alpha = \tan^{-1}\left(\frac{\partial z}{\partial x}\right)$ and c is the chord length of camber line nondimensionalized with respect to the chord, and δ_x to δ_z evaluated at the leading edge. The integrals in equation (13)-(15) can be evaluated by midpoint trapezoidal rule in the θ - plane as illustrated in equation (7). The above formulation can be easily shown to be consistent with the exact theory for a flat-plate airfoil. For example, with $\frac{\partial z}{\partial x} = 0$ in equation (10) the solution obtained is the well known $\Delta C_l = 4\sqrt{(1-\xi)/\xi}\sin\alpha$ and hence $c_a = 2\pi\sin^2\alpha$. It follows that

$$c_n = 2\pi\sin\alpha\cos^2\alpha + 2\pi\sin^2\alpha\sin\alpha = 2\pi\sin\alpha \tag{16a}$$

$$c_{a_1} = 2\pi\cos\alpha\sin^2\alpha - 2\pi\sin^2\alpha\cos\alpha = 0 \tag{16b}$$

$$c_{m_0} = -\frac{\pi}{2}\sin\alpha\cos\alpha \tag{16c}$$

Flapped

The method described above can be extended to airfoils with flap deflection. In this case, the distribution of pressure points and [illegible] on the airfoil and the flap will be given separately by the cosine spacing, following the QVLM (ref. 7). For a flat airfoil with flap deflection δ_f, the exact linear solution is given by (ref. 8):

$$\Delta C_p(\xi) = 4\alpha\sqrt{\frac{1-\xi}{\xi}} + 4\frac{\delta_f}{\pi}\left(\tau\sqrt{\frac{1-\xi}{\xi}} + \ln\left|\frac{\sin\frac{\phi+\tau}{2}}{\sin\frac{\phi-\tau}{2}}\right|\right) \tag{17a}$$

$$c_\ell = 2\pi\alpha + 2\delta_f(\tau + \sin\tau) \tag{17b}$$

$$c_{m_{l.e.}} = -\frac{\pi}{2}\alpha - \delta_f\left(\frac{\tau}{2} + \sin\tau + \frac{\sin(2\tau)}{4}\right) \tag{17c}$$

where

$$\cos\phi = 2\xi - 1 \tag{17d}$$

$$\cos\tau = 2\xi_f - 1$$

and ξ_f is the flap hinge location. Using equation (17a) for the ΔC_p, the correct control points can again be obtained through iteration. It should be noted that in general the iterative method to find the correct control points for a flapped airfoil may not converge, as some control points may move out of the corresponding panels at some iterative steps. When this happens, that particular control point is reset at 95% of the panel chord before the iteration is resumed. The correct set of control points is taken to be the one with least square difference of Δc_p between exact and calculated distribution.

Wings

For three-dimensional wings with straight leading edges, the chordwise distribution of control points and panels follows directly from the two-dimensional theory described above. The spanwise distribution of control stations and panel widths is based on that used in the MCAIR (ref. 7) in accordance with the leading edge. The control stations are given by

$$y_i = (b/2)[1 - \cos(i\pi/(N_s + 1))]/2, \quad i=1, \ldots, N_s \tag{19}$$

and the strip widths are given by

$$y_j = (b/2)[1 - \cos((2j - 1)\pi/2(N_s + 1))]/2, \quad j=1, \ldots, N_s + 1 \tag{20}$$

where N_s is the number of spanwise strips. The inboard gap created by the scheme given by equation (20) should be eliminated, and the tip inset from equation (20) is retained, as described in reference 7. In general, the control stations will not pass through the panel centroids. From extensive calculation, the chosen spanwise paneling scheme appears to be the best for calculating the side-edge suction force.

Once the pressure distribution is obtained, the interpolation by Fourier series is used to find the distribution of the leading-edge suction, the streamwise vortex density, γ_x, and the side-edge suction. For example, to find the leading-edge suction parameter C, ΔC_p is first multiplied by $\frac{1}{2}\sin\theta$ and then developed in a cosine Fourier series:

$$f(\theta) = \frac{1}{2}\Delta C_p \sin\theta = a_0 + \sum_{j=1}^{N_c} a_j \cos j\theta \tag{21}$$

where the Fourier coefficients a_j can be computed by midpoint trapezoidal rule in terms of ΔC_p as follows:

$$a_0 = \frac{1}{\pi}\int_0^{\pi} f(\theta)d\theta = \frac{1}{N_c}\sum_{k=1}^{N_c} f(\theta_k) \qquad (3a)$$

$$a_j = \frac{2}{\pi}\int_0^{\pi} f(\theta)\cos j\theta d\theta = \frac{2}{N_c}\sum_{k=1}^{N_c} f(\theta_k)\cos j\theta_k \qquad (3b)$$

Near the leading edge, $\Delta C_p = C\sqrt{(1-x)/x}$. Hence,

$$\lim_{x\to 0}\frac{1}{2}\Delta C_p \sin\theta = C = a_0 + \sum_{j=1}^{N_c} a_j \qquad (3c)$$

The sectional leading edge suction is then given by (ref. 7)

$$c_s = (\pi/8)C^2(1-M_\infty^2\cos^2\Lambda_{L.E.})^{1/2}/\cos^2\Lambda_{L.E.} \qquad (4)$$

The side-edge suction per unit length of the tip chord is given by (see ref. 9)

$$s_t(x) = \pi\rho G^2(x) \qquad (5)$$

where $G(x)$ is defined by

$$G(x) = \int_{y}^{\frac{b}{2}} \lim_{y\to b/2}\sqrt{1 - y/(b/2)}\;\frac{1}{2}\gamma_x \qquad (6)$$

To find γ_x, the conservation of vorticity is used:

$$\frac{\partial \gamma_x}{\partial x} + \frac{\partial \gamma_y}{\partial y} = 0 \tag{27}$$

If $\Gamma(x,y)$ is defined as

$$\Gamma(x,y) = -\int_{x_\ell}^{x} \gamma_y(x',y)dx' \tag{28}$$

equation (27) can be shown to give

$$\gamma_x = \frac{\partial \Gamma(x,y)}{\partial y} \tag{29}$$

In the linear theory, $\gamma_y = \Delta C_p/2$. Hence, equation (28) can be written as

$$\Gamma(x,y) = -\frac{c(y)}{2}\int_0^\theta \frac{1}{2}\Delta C_p \sin\theta d\theta \tag{30}$$

Using equation (21), equation (30) can be integrated in closed form. The differentiation in equation (29) is performed through the use of trigonometric interpolation formula. The detail can be found in reference 6.

As can be seen from the above description, not only the leading-edge and side-edge suction forces can be predicted by the method, but also the distribution of γ_x which is needed in calculating some lateral-directional stability derivatives.

NUMERICAL RESULTS AND DISCUSSIONS

Airfoils

For a flat-plate airfoil in incompressible flow, all aerodynamic characteristics of interest can be exactly predicted by the present method.

The computed control points are in general located at 81.5% for the leading-edge panel and moved to 97.2% for the trailing-edge panel. For a cambered airfoil with or without flap deflection, only approximate results can be calculated. Figure 2 shows the comparison of the present predicted pressure distribution for a circular-arc airfoil with the results by conformal mapping (ref. 10). The lift coefficient and the center of pressure are presented in Table 1. It is seen that the present results are quite accurate. The indication of accuracy of the method is the magnitude of the calculated induced drag coefficient. The exact potential-flow solution is $c_{d_i} = 0$. For the circular-arc airfoil with $h/c = 0.0314$ as shown in figure 2, the calculated c_{d_i} is about 0.1% of c_ℓ. It becomes 0.2% of c_ℓ when h/c is increased to 0.20.

The predicted pressure distribution for a flapped airfoil with flap chord ratio of 0.30, $\delta_f = 40°$ and $\alpha = 10°$ is presented in figure 3. Also shown is the result by the original Woodward's method, in which uniform panel size on the airfoil and flap is assumed. The calculated ΔC_p is assumed to be at the panel midpoint. In both the original and the improved methods, seven and four panels are used on the airfoil and flap, respectively. The calculated c_ℓ and $c_{m_{\ell e}}$ are also presented in Table 1. The discrepancy in the calculated c_ℓ and c_m by the present method and the exact solution, as given in Table 1, is mainly due to the quadrature method used (i.e. midpoint trapezoidal rule) in integrating the pressure force. The method, which is also used in the QVLM, cannot account exactly for the logarithmic singularity in the ΔC_p distribution. Although the original Woodward's method can predict c_ℓ and c_m reasonably well (see Table 1), the calculated pressure distribution is inaccurate near the flap

hinge, as shown in figure 3. Note the present method and exact solution are in excellent agreement, to the extent, that the dashed curve cannot be distinguished from the solid curve.

Wings

In three-dimensional cases, it is assumed that the control point locations obtained from the two-dimensional theory are directly applicable. One important application of calculating leading-edge and side-edge suction forces is the prediction of vortex lift through Polhamus' method of suction analogy as extended in reference 9. According to this method, the total lift coefficient for a flat wing exhibiting edge-separated vortex flow can be written as

$$C_L = K_p \sin\alpha\cos^2\alpha + (K_{v,le} + K_{v,se}) \sin^2\alpha\cos\alpha \qquad (31)$$

where the lift factors K_p, $K_{v,le}$ and $K_{v,se}$ are the lift curve slope per radian and the leading-edge and the side-edge suction coefficients at one radian of angle of attack, respectively, from linear potential theory.

To validate the present method, extensive comparisons will be made of the predicted K_p, $K_{v,le}$ and $K_{v,se}$ with other theoretical results. Furthermore, from convergence studies with the present method, it was determined that solutions converged rapidly with increasing number of panels. For example, with eight or nine chordwise panels and 10 to 15 spanwise strips, aerodynamic characteristics of simple planforms can be accurately calculated with confidence. Further increase in the number of strips will not change the calculated results significantly. The results to be presented below were mostly obtained with nine chordwise elements and 12 spanwise strips, except those cases when the pressure distribution is desired.

In these cases, 13 spanwise strips were used. Since the chordwise control-point locations are based on the two-dimensional incompressible flow theory, any deviation of the pressure distribution from the two-dimensional theory will lead to some inaccuracy of the method. This appears to be the cause in predicting $K_{v,\ell e}$ for highly swept planforms in subsonic and supersonic flow with leading-edge sweep angle $\geq 60^\circ$. In both situations, the predicted $K_{v,\ell e}$ was found to be slightly too high. This problem has been alleviated empirically by moving downstream the control points of the leading-edge panels by a certain percent, Δ, of the elemental panel chord, where,

for $M < 1$, $\quad \Delta = 0 \quad$ for $\Lambda \leq 60^\circ$

$\Delta = 0.35\,(\Lambda - 60) \quad$ for $\Lambda > 60^\circ$

for $M \geq 1$, $\quad \Delta = 3.0 \quad$ for $\Lambda \leq 60^\circ$

$\Delta = 3.0 + 0.35\,(\Lambda - 60) \quad$ for $\Lambda > 60^\circ$

For cranked wings also, a uniform constant percent chordwise location for the first control point is used all across the span for simplicity. The sweep angle for determining its location is obtained by weighting the sweep angles with respect to the length of the leading-edges of each section.

Typical pressure distributions in supersonic flow are presented in figures 4 and 5 and are compared with the exact solution obtained from reference 11. The most visible improvement in the predicted pressure distribution appears to be over the inboard section. To improve the predicted pressure distribution in the tip region, it was found that the number of spanwise strips has to be further increased. However, the inaccuracy in the predicted pressure distribution in the tip region apparently does not affect the accuracy of the overall force coefficients because of the decreasing chord. The lift factors K_p, $K_{v,\ell e}$ and $K_{v,le}$ for the rectangular wing of aspect ratio 2.0 are presented in figure 6 as a function of Mach number and tabulated also in Table 2. The agreement of the present results with

Lamar's (ref. 9) in subsonic flow is excellent. This is particularly true in K_p and $K_{v,\ell e}$ prediction in that the present results are indistinguishable from Lamar's. The supersonic results also agree well with the exact linear theory (ref. 12 and 13). Note that the original Woodward's method tends to predict higher K_p.

The results for a cropped delta wing of low aspect ratio are presented in figure 7 and Table 3. The agreement with other theoretical results appears to be reasonably good, except that the predicted $K_{v,\ell e}$ in subsonic flow are slightly higher than those given by Multhopp's method of Lamar (ref. 9). (The effect of Mach number on $K_{v,se}$ was first shown for these two wings in reference 14).

The sectional leading-edge and wing-tip suction coefficients for cropped delta wings are plotted in figures 8 and 9 at Mach numbers 0 and 1.8. At both Mach numbers the sectional leading-edge suction coefficients agree very well with other methods (refs. 7, 9, 11 and 15) in the inboard region. The agreement is not as good in the tip region. With regard to the wing-tip suction coefficients, at subsonic speed the present method is in good agreement with that of Lamar (ref. 9). At both subsonic and supersonic speeds the present method shows an overshoot near the leading-edge caused by the method trying to represent the exact continuous solution with finite panels.

Additional comparisons for various configurations are presented in Table 4. The planform shapes used in comparison include straight, tapered wings and a family of double delta configurations of reference 16 which are illustrated in figure 10. The results indicate that the present method can predict edge suction force values that are in reasonable agreement with other methods, even for complex planforms.

So far only the lift factors and pressure distributions have been compared. The centers of these forces can also be accurately predicted. According to the method of suction analogy, the pitching moment of wings with edge-separated vortex flow can be calculated as (ref. 9):

$$C_m = \left[K_p \sin\alpha\cos\alpha \frac{\bar{x}_p}{c_r} + K_{v,\ell e} \sin^2\alpha \frac{\bar{x}_{\ell e}}{c_r} + K_{v,se} \sin^2\alpha \frac{\bar{x}_{se}}{c_r}\right] \frac{c_r}{c_{ref}} \qquad (3.4)$$

The calculation of the center-of-force factors $\bar{x}_p$, $\bar{x}_{\ell e}$ and $\bar{x}_{se}$ is compared in Table 5 for the cropped delta wing of figure 7. The results indicate that the centers of edge suction forces are well predicted by the present method.

CONCLUSIONS

Based on the extensive comparison of present prediction with other theoretical results, it may be concluded that the present improved Woodward panel method is generally accurate in predicting the leading-edge and side-edge suction forces and the centers of these forces in subsonic and supersonic flow. The good accuracy of the present method has also been demonstrated for cambered and flapped airfoils. Because of generality of the panel method, the present improved method can therefore be used not only to predict the vortex lift of complex planforms through the method of suction analogy, but also to calculate certain lateral-directional stability derivatives as well.

REFERENCES

(1) Woodward, F. A., "Analysis and Design of Wing-Body Combinations at Subsonic and Supersonic Speeds," Journal of Aircraft, Vol. 5, Nov.-Dec. 1968, pp. 528-534.

(2) Lan, C. and Roskam, J., "Leading-Edge Force Features of the Aerodynamic Finite Element Method," Journal of Aircraft, Vol. 9, Dec. 1972, pp. 864-867.

(3) Carmichael, R. L., Castellano, C. R. and Chen, C. F., "The Use of Finite Element Methods for Predicting the Aerodynamics of Wing-Body Combinations," Discussions by J. P. Giesing, NASA SP-228 Analytic Methods in Aircraft Aerodynamics, 1969.

(4) Hink, G. R., et al., "A Method for Predicting the Stability Characteristics of Control Configured Vehicles. Vol. II - FLEXSTAB User's Manual," Air Force Flight Dynamics Laboratory, Wright-Patterson Air Force Base, Ohio, Rept. AFFDL-TR-74-91, Nov. 1974.

(5) Dillenius, M. F. E. and Nielsen, J. N., "Prediction of Aerodynamics of Missiles at High Angles of Attack in Supersonic Flow," Nielsen Engineering and Research, Inc., Mountain View, Ca., Rept. NEAR TR-99, Oct. 1975.

(6) Lan, C. E., "Calculation of Lateral-Directional Stability Derivatives for Wing-Body Combinations With and Without Jet Interaction Effects," NASA CR-145251, 1977.

(7) Lan, C. E., "A Quasi Vortex-Lattice Method in Thin Wing Theory," Journal of Aircraft, Vol. 11, Sept. 1974, pp. 518-527.

(8) Spence, D. A., "The Lift on a Thin Aerofoil with a Jet-Augmented Flap," Aeronautical Quarterly, Vol. 9, Aug. 1958, pp. 289-299.

(9) Lamar, J. E., "Extension of Leading-Edge-Suction Analogy to Wings with Separated Flow Around the Side Edges at Subsonic Speeds," NASA TR R-428, October 1974.

(10) Lamar, J. E., "Nonplanar Method for Predicting Incompressible Aerodynamic Coefficients of Rectangular Wings with Circular-Arc Camber," NASA TMX-67791, December 1971.

(11) Malvestuto, F. S. Jr., Margolis, K. and Ribner, H. S., "Theoretical Lift and Damping in Roll of Thin Sweptback Wings of Arbitrary Taper and Sweep at Supersonic Speeds. Subsonic Leading Edges and Supersonic Trailing Edges," NACA TN 1860, April 1949.

(12) Margolis, K., "Theoretical Calculations of the Lateral Forces and Yawing Moment Due to Rolling at Supersonic Speeds for Sweptback Tapered Wings with Streamwise Tips. Subsonic Leading Edges," NACA TN 2122, June 1950.

(13) Harmon, S. M., "Stability Derivatives at Supersonic Speeds of Thin Rectangular Wings with Diagonals Ahead of Tip Mach Lines," NACA Report 925, 1949.

(14) Lamar, J. E., "Some Recent Applications of the Suction Analogy to Vortex-Lift Estimates," NASA SP-347, March 1975.

(15) Lamar, J. E. and Gloss, B. B., "Subsonic Aerodynamic Characteristics of Interacting Lifting Surfaces with Separated Flow Around Sharp Edges Predicted by a Vortex-Lattice Method," NASA TND-7921, Sept. 1975.

(16) Lamar, J. E., "Strake-Wing Analyses and Design," AIAA Paper 78-1201, July 1978.

Table 1. Predicted Aerodynamic Characteristics for Cambered and Flapped Airfoils

Airfoil	Aerodynamic variable	Exact	Present	Woodward (ref. 1)
circular-arc, with h/c = 0.0314 $\alpha = 0^{\circ}$	c_{ℓ}	(ref. 10) 0.941	0.9345	Not Determined
	x_{cp}	0.355	0.35575	"
Flat Airfoil with 30 deg. Flap and Flap Chord Ratio = 0.30, $\alpha = 10^{\circ}$	c_{ℓ}	(ref. 8) 3.265	3.30	3.212
	$c_{m_{\ell e}}$	-1.152	-1.175	-1.142

Table 2. Comparison of Predicted Lift Factors for a Rectangular Wing of A = 2.0

M	K_p				$K_{v,le}$		$K_{v,se}$		
	Present	Lamar (ref. 9)	Woodward (ref. 1)	Exact (ref. 13)	Present	Lamar (ref. 9)	Present	Lamar (ref. 9)	Exact (ref. 12)
0.	2.4783	2.4763	2.5744	Not Available	1.4991	1.4997	1.5793	1.5489	Not Available
0.2	2.4956	2.4934	2.5928	"	1.5027	1.5033	1.5978	1.5673	"
0.4	2.5507	2.5479	2.6514	"	1.5136	1.5142	1.6582	1.6272	"
0.6	2.6553	2.6517	2.7627	"	1.5313	1.5323	1.7804	1.7483	"
0.8	2.8389	2.8354	2.9592	"	1.5537	1.5558	2.0292	1.9939	"
0.9	2.9811	2.9783	3.1126	"	1.5634	1.5665	2.2791	2.2354	"
1.1	3.7943	-	4.0393	"	0.	-	2.5737	-	"
1.2	3.6321	-	3.8114	3.7575	0.	-	1.8664	-	"
1.4	2.9864	-	3.0975	3.0408	0.	-	1.2647	-	"
1.6	2.5304	-	2.6129	2.5615	0.	-	0.9929	-	1.0194
1.8	2.2062	-	2.2725	2.2262	0.	-	0.8301	-	0.8507
2.0	1.9630	-	2.0181	1.9760	0.	-	0.7190	-	0.7351

Table 3. Comparison of Predicted Li t Factors for a Cropped Delta Wing

$A = 0.874$, $\lambda = 0.4$ and $\Lambda = 63^{\circ}$

M	K_p			$K_{v,le}$			$K_{v,sc}$		
	Present	Lamar (ref. 9)	Woodward (ref. 1)	Present	Lamar (ref. 9)	Exact (ref. 12)	Present	Lamar (ref. 9)	Exact (ref. 12)
0.	1.2968	1.2789	1.3632	1.5297	1.5041	Not Available	1.4325	1.3967	Not Available
0.2	1.2999	1.2819	1.3667	1.5315	1.5046	"	1.4408	1.4039	"
0.4	1.3095	1.2911	1.3774	1.5371	1.5059	"	1.4673	1.4262	"
0.6	1.3263	1.3073	1.3963	1.5473	1.5078	"	1.5164	1.4662	"
0.8	1.3517	1.3326	1.4253	1.5647	1.5099	"	1.6004	1.5288	"
0.9	1.3679	1.3500	1.4440	1.5790	1.5107	"	1.6668	1.5707	"
1.2	1.5247	-	1.6330	1.0504	-	"	2.0902	-	"
1.4	1.6140	-	1.7129	0.8407	-	"	2.0483	-	"
1.6	1.6113	-	1.6973	0.6668	-	0.6885	1.9493	-	2.0749
1.8	1.5732	-	1.6495	0.5084	-	0.5055	1.8400	-	1.9263
2.0	1.5225	-	1.5892	0.3606	-	0.3244	1.7200	-	1.8036
2.2	1.4583	-	1.5166	0.0242	-	0.0337	1.5514	-	1.6989
2.4	1.3859	-	1.4404	0.	-	0.	1.3515	-	1.6079

BLANK

PAGE

Table 5. Comparison of Predicted Center-of-Force Factors for a Cropped Delta Wing. $A = 0.874$, $\Lambda = 63^{\circ}$, $\lambda = 0.4$. (Reference Point at the Leading Edge of Root Chord).

M	$-\bar{x}_p/c_r$		$-\bar{x}_{le}/c_r$		$-\bar{x}_{se}/c_r$	
	Present	ref. 9	Present	ref. 9	Present	ref. 9
0.	0.4228	0.4353	0.3512	0.3576	0.8128	0.8150
0.2	0.4226	0.4355	0.3519	0.3582	0.8126	0.8148
0.4	0.4217	0.4361	0.3544	0.3601	0.8119	0.8144
0.6	0.4197	0.4378	0.3589	0.3631	0.8106	0.8137
0.8	0.4156	0.4428	0.3668	0.3658	0.8082	0.8129
0.9	0.4111	0.4501	0.3730	0.3631	0.8061	0.8129
- - -	- - - - - - - - - - - - - - -		- - - - - - -	Exact (ref. 12)	- - - - - -	Exact (ref. 12)
1.8	0.5295	Not Determined	0.3932	0.40	0.8082	0.8095
2.0	0.5401	"	0.3967	0.40	0.8107	0.8095

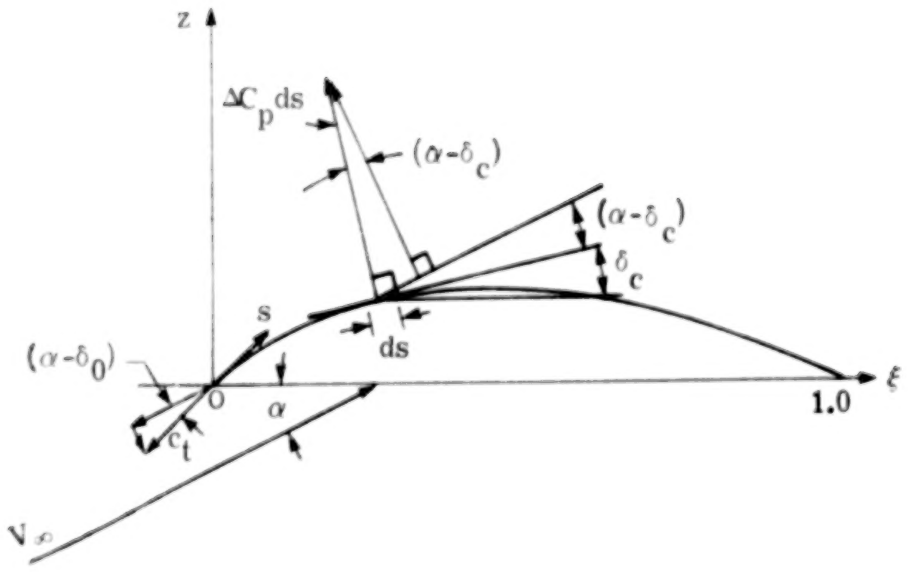

Figure 1.- Resolution of Forces for Cambered Airfoils.

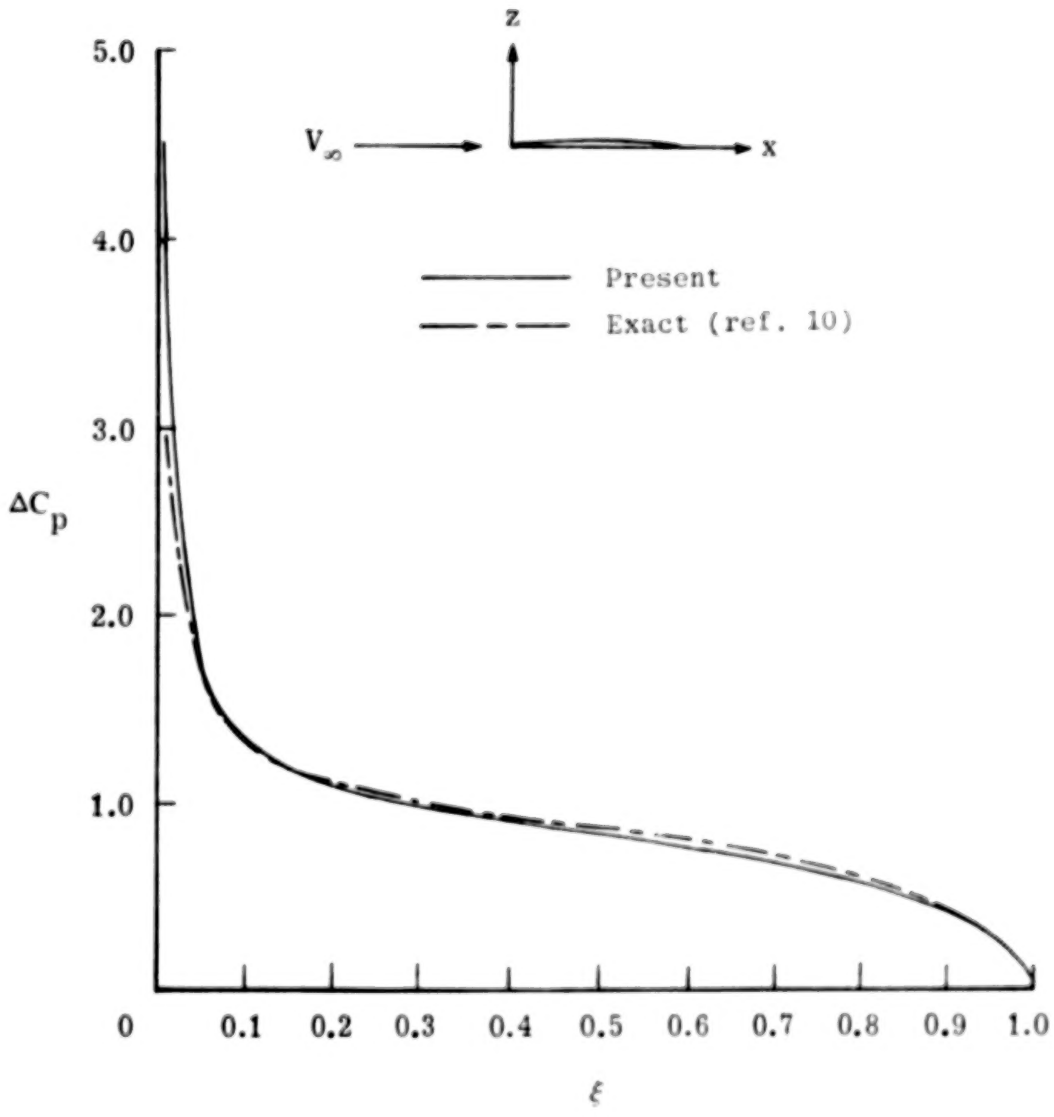

Figure 2.- Predicted Pressure Distributions for Circular Arc Airfoil, h/c = 0.0314, α = 0.0 deg.

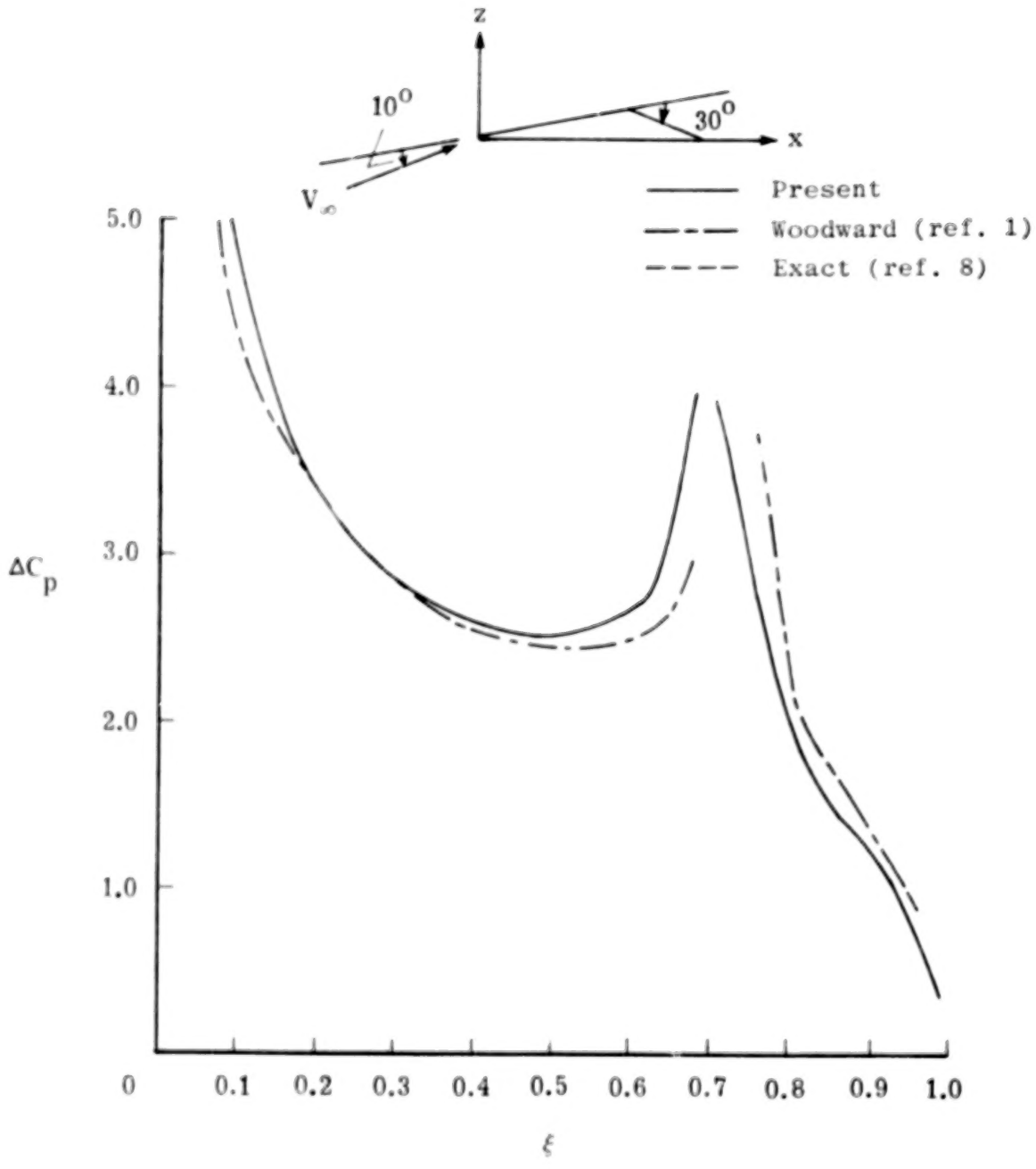

Figure 3.- Predicted Pressure Distributions for Flat-Plate Airfoil with Flap Angle of 30 deg. Flap-Chord Ratio = 0.30, α = 10 deg.

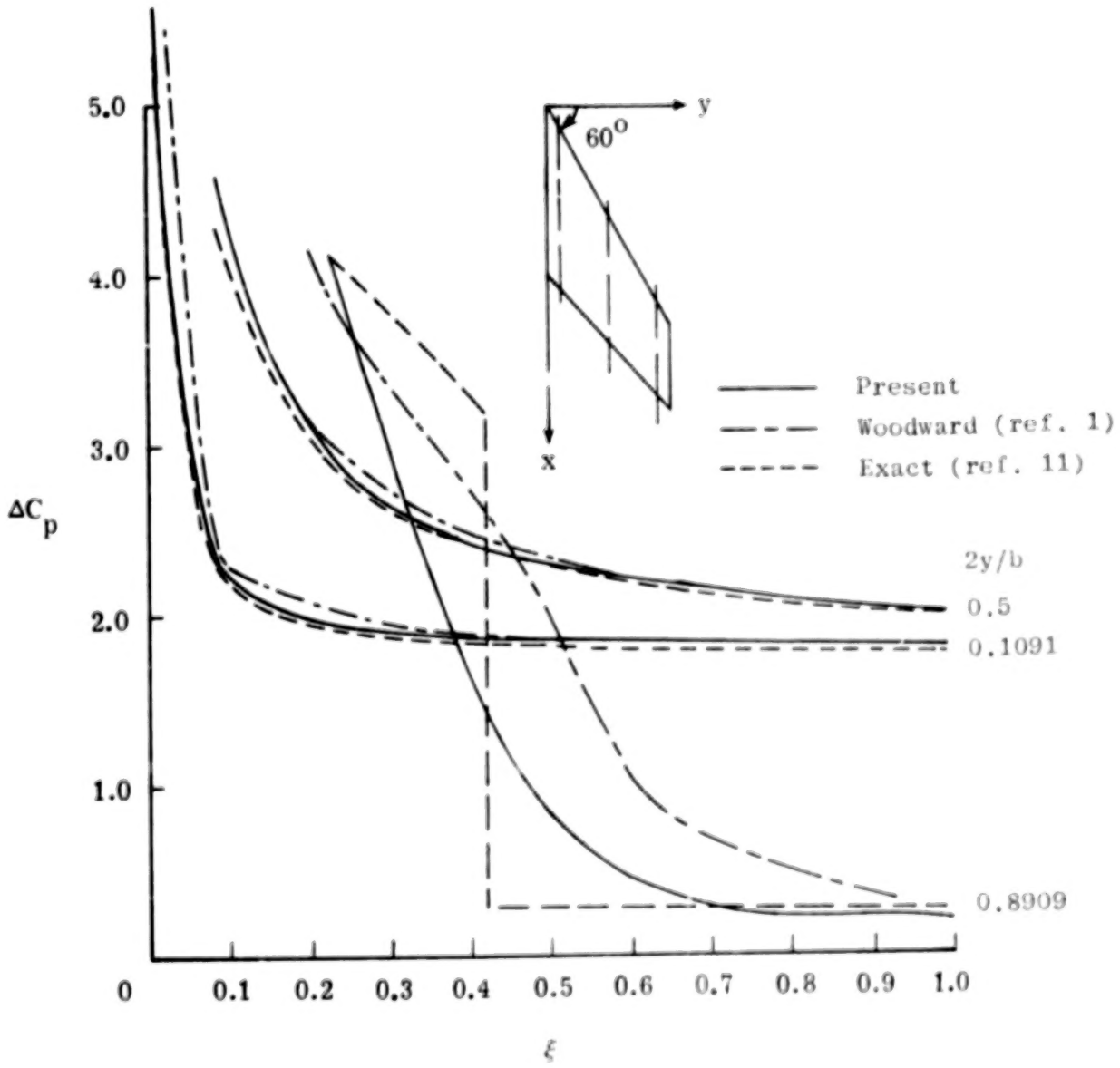

Figure 4.- Predicted Pressure Distributions for Cropped Arrow Wing of A = 2.0, λ = 0.5 at M = 1.5 and α = 1.0 Radian.

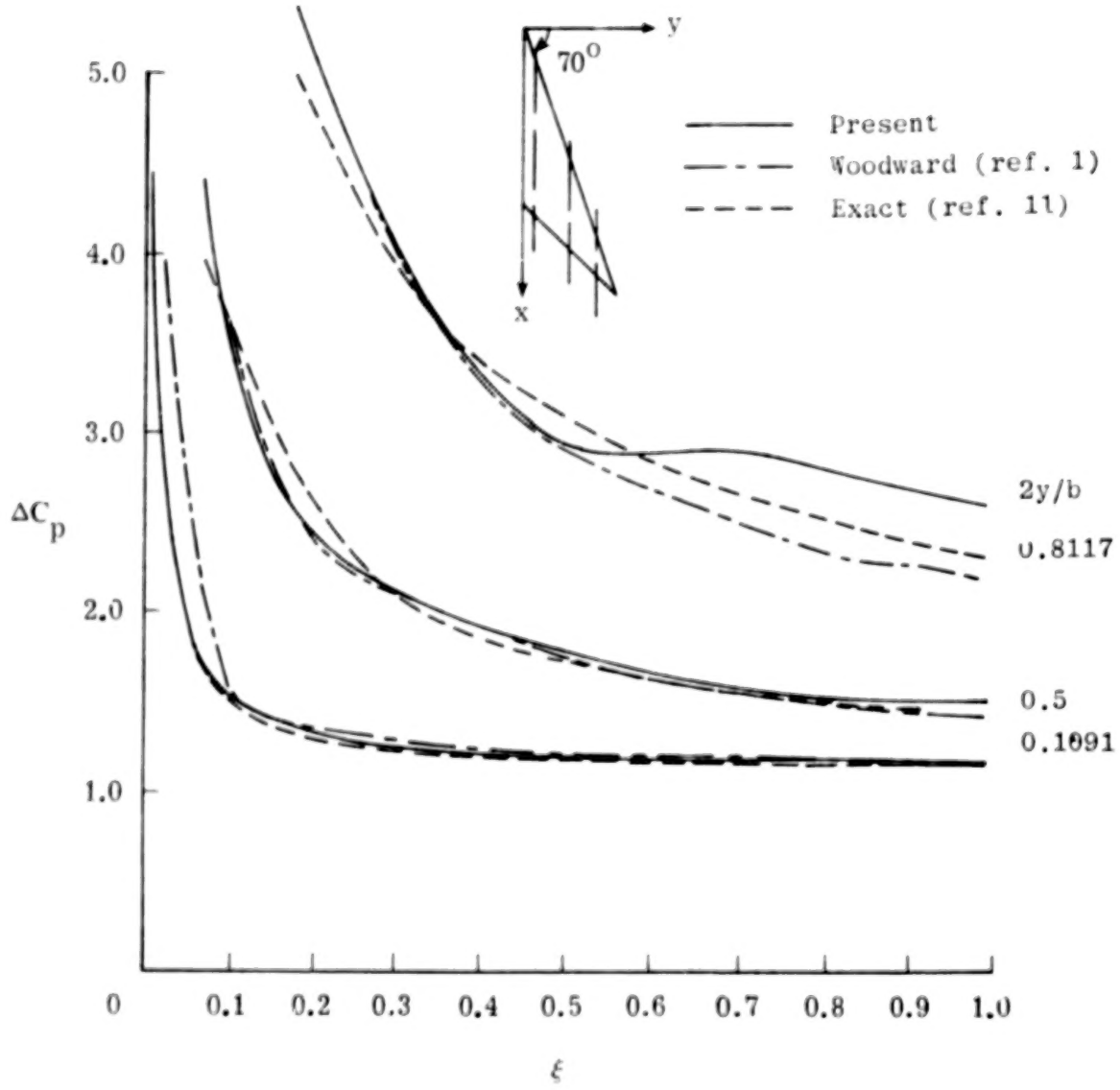

Figure 5.- Predicted Pressure Distributions for Arrow Wing of A = 2.24 at M = 2.0 and α = 1.0 Radian.

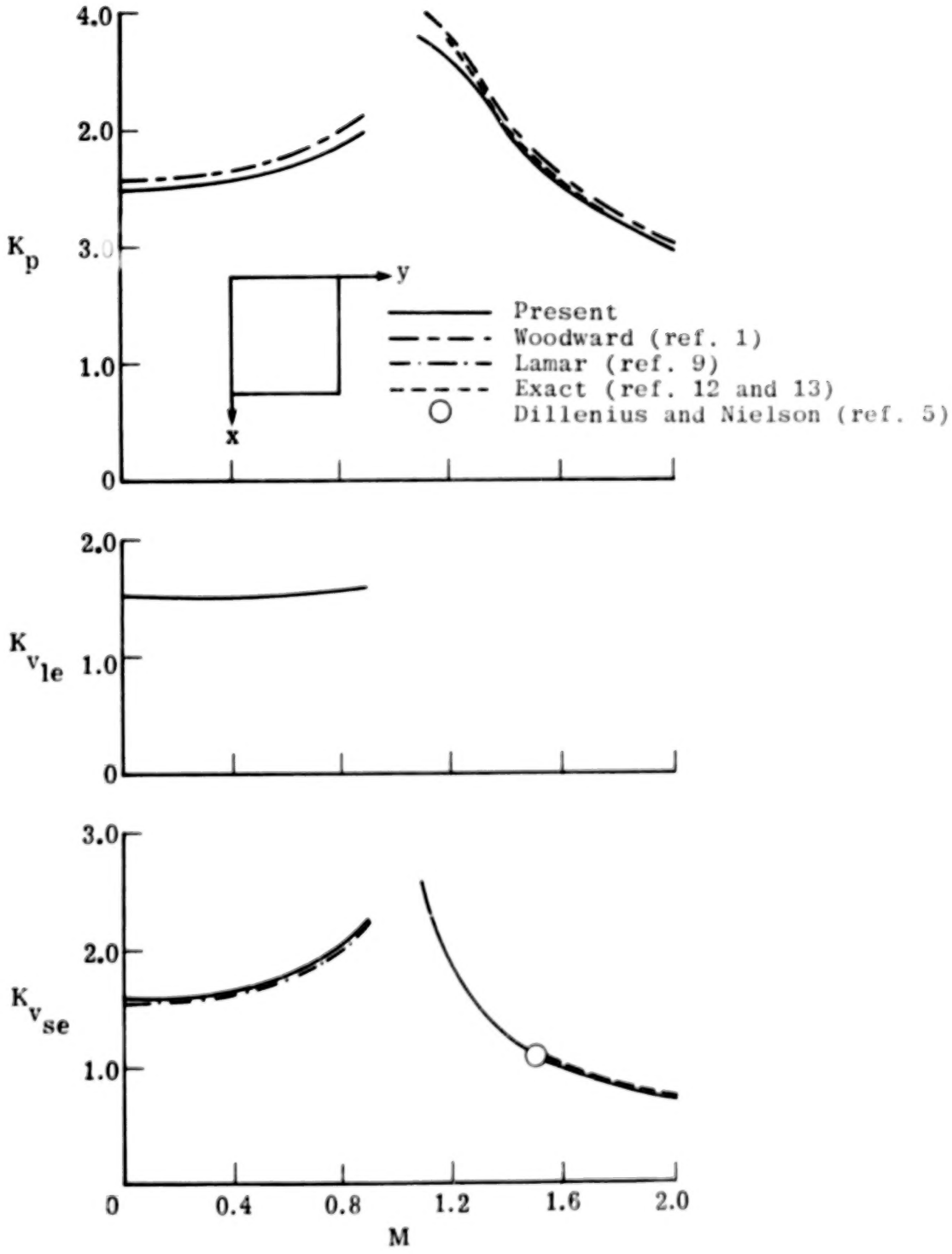

Figure 6.- Predicted Lift Factors for Rectangular Wing of A = 2.0.

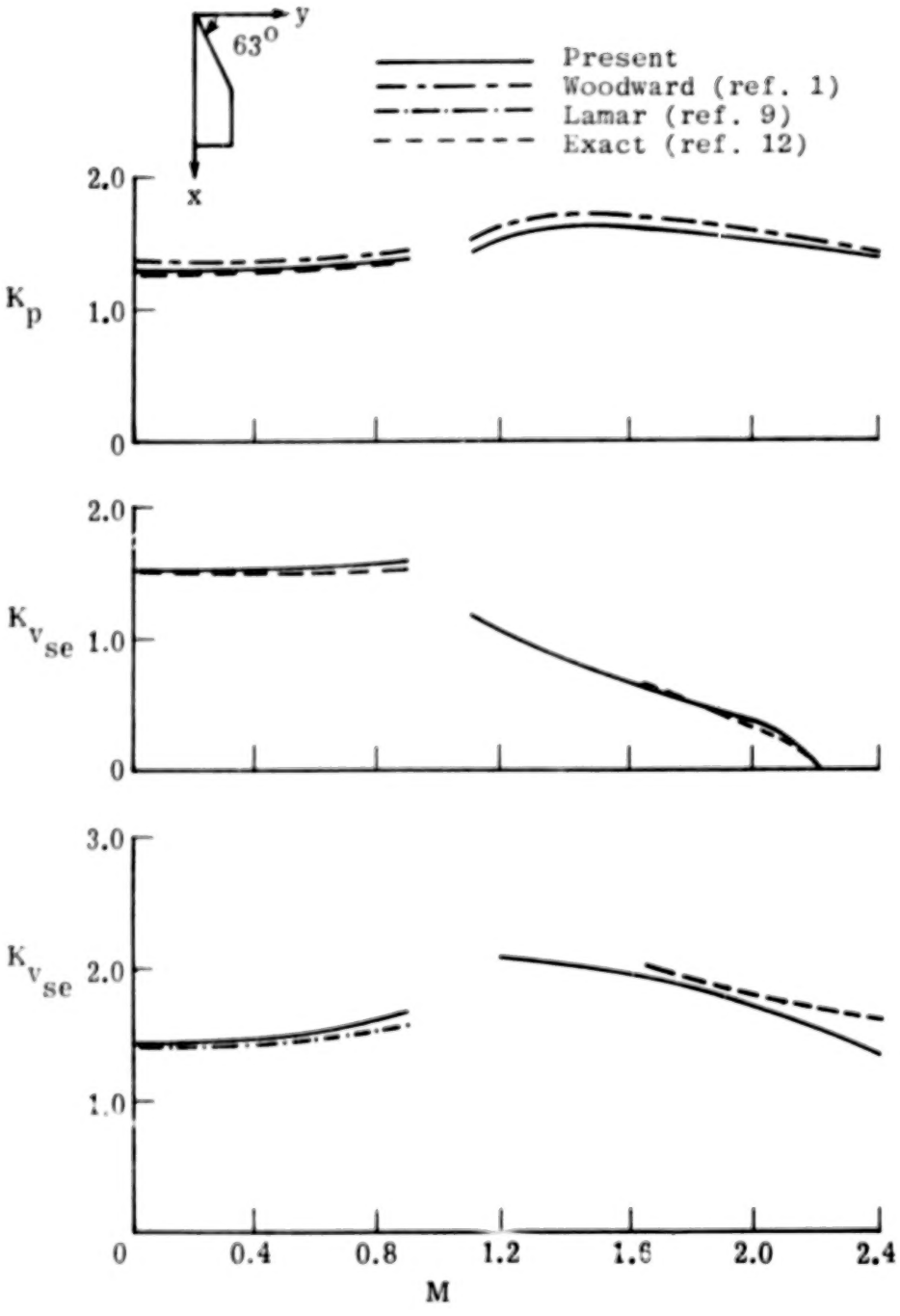

Figure 7.- Predicted Lift Factor for Cropped Delta Wing of A = 0.874 and λ = 0.4.

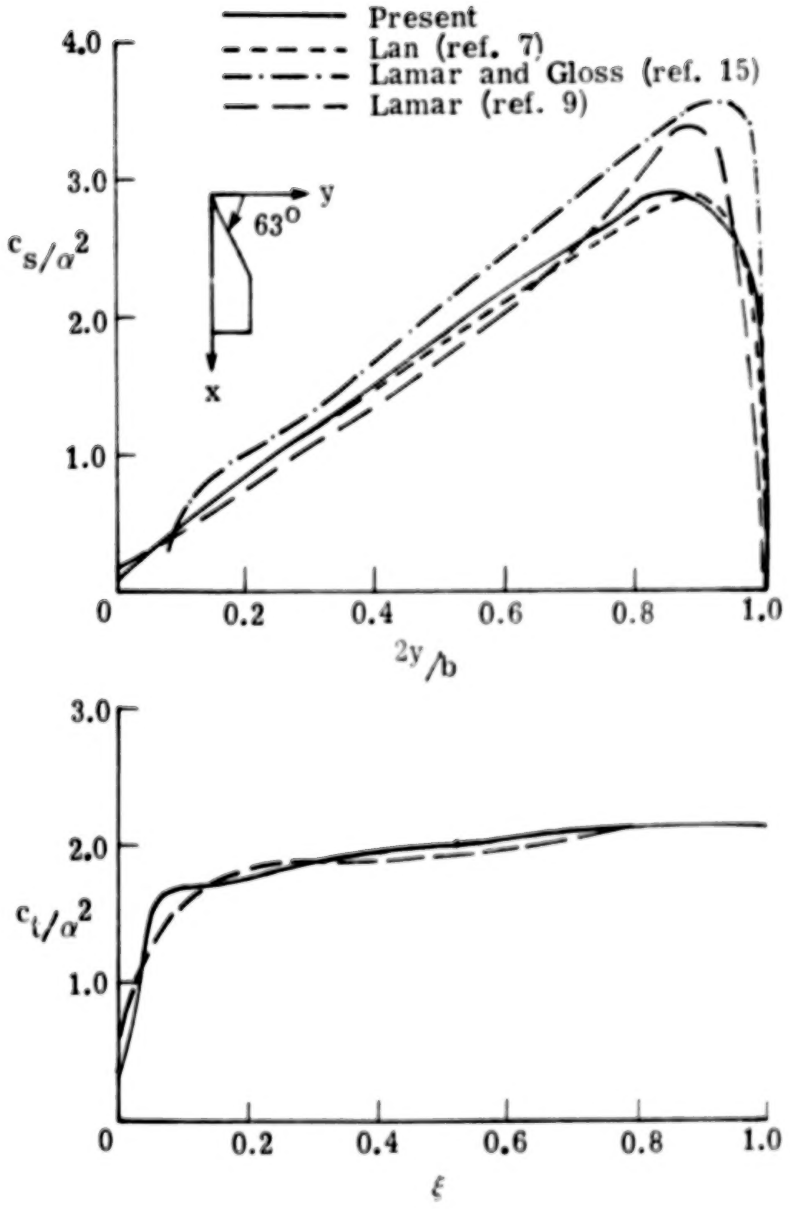

Figure 8.- Distribution of Leading Edge and Wing-Tip Suction Coefficients for Cropped Delta Wing of A = 0.874 and λ = 0.4 at M = 0.

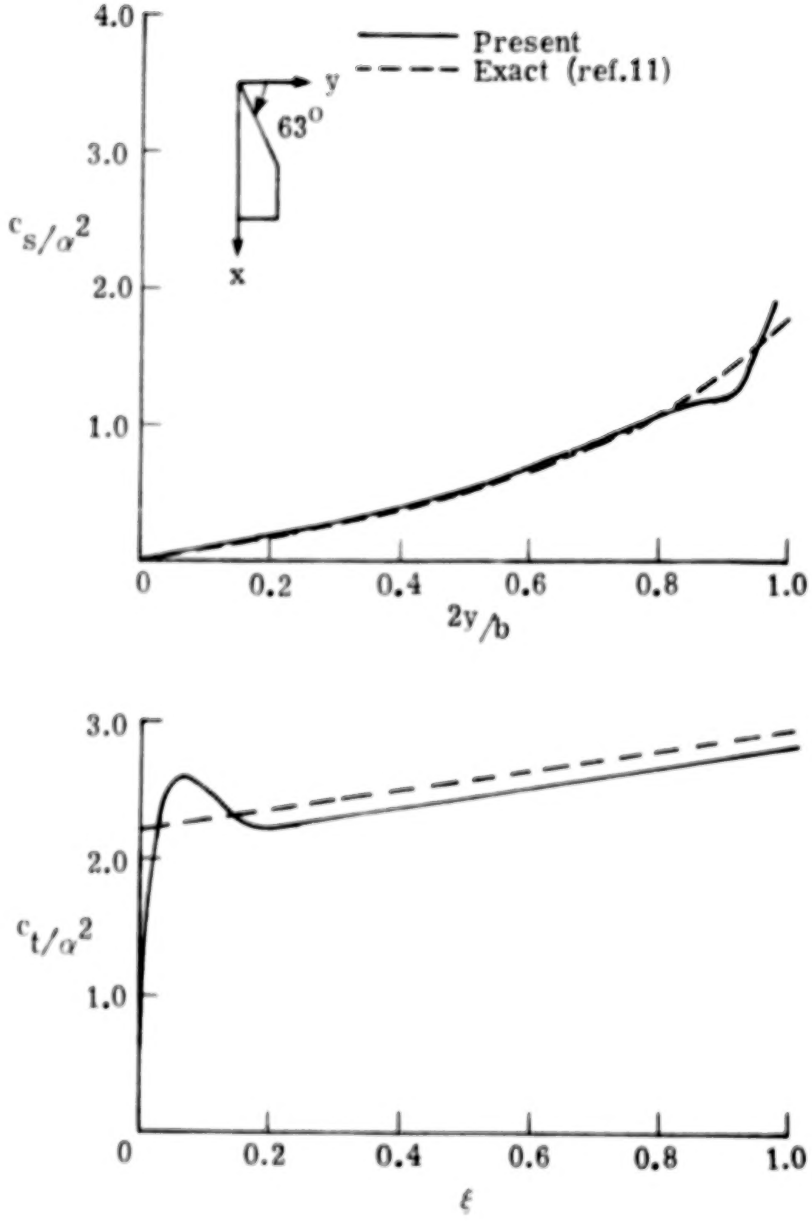

Figure 9.- Distribution of Leading Edge and Wing-Tip Suction Coefficients for Cropped Delta Wing of A = 0.874 and λ = 0.4 at M = 1.8.

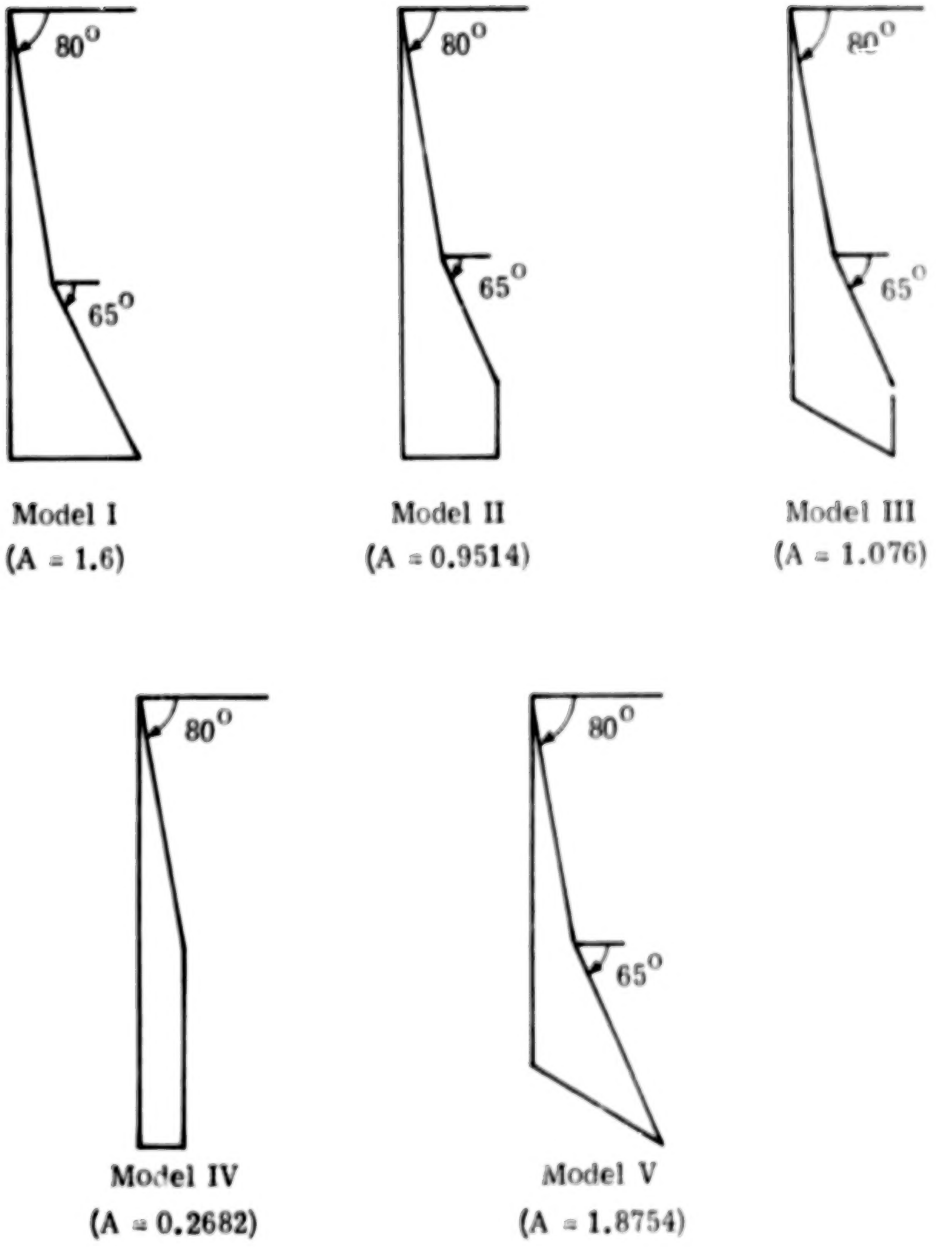

Figure 10.- Geometry of Family of Double Deltas of Reference 16 and Referred in Table 4.

1 Report No.	2 Government Accession No.	3 Recipient's Catalog No.
NASA CR-3205		

4 Title and Subtitle	5 Report Date
AN IMPROVED WOODWARD'S PANEL METHOD FOR CALCULATING LEADING-EDGE AND SIDE-EDGE SUCTION FORCES AT SUBSONIC AND SUPERSONIC SPEEDS	November 1979
	6 Performing Organization Code

7 Author(s)	8 Performing Organization Report No.
C. Edward Lan and Sudhir C. Mehrotra	CRINC-FRL-266-3
	10 Work Unit No. 505-11-13-03

9 Performing Organization Name and Address	11 Contract or Grant No.
The University of Kansas Center for Research, Inc. Lawrence, Kansas 66045	
	13 Type of Report and Period Covered: Contractor Report

12 Sponsoring Agency Name and Address	14 Sponsoring Agency Code
National Aeronautics and Space Administration Washington, DC 20546	

15 Supplementary Notes
Langley Technical Monitor: John E. Lamar
Topical Report

16 Abstract
Woodward's panel method for subsonic and supersonic flow is improved by employing control points determined by exactly matching two-dimensional pressure at a finite number of points. The results show great improvement in the predicted pressure distribution of a flapped airfoil. With the paneling scheme of cosine law in both chordwise and spanwise directions, the method is shown to accurately predict leading-edge and side-edge suction forces of various configurations in subsonic and supersonic flow.

17 Key Words (Suggested by Author(s))	18 Distribution Statement
Leading-Edge Suction Side-Edge Suction Aerodynamic Characteristics Pressure Distribution Lift Factors	Unclassified - Unlimited Star Category 02

19 Security Classif. (of this report)	20 Security Classif. (of this page)	21 No. of Pages	22 Price*
Unclassified	Unclassified	34	$4.50

* For sale by the National Technical Information Service, Springfield, Virginia 22161

NASA-Langley, 1979

90%

END